PNAS RESEARCH ARTICLE | MICROBIOLOGY OPEN ACCESS

# *Staphylococcus aureus* induces a muted host response in human blood that blunts the recruitment of neutrophils

Erin E. Zwack[a,1], Ze Chen[a,1], Joseph C. Devlin[a,1,2], Zhi Li[b,3], Xuhui Zheng[a], Ada Weinstock[c,5], Keenan A. Lacey[a], Edward A. Fisher[a,c], David Fenyö[b,d], Kelly V. Ruggles[b,e,4], P'ng Loke[a,f,4], and Victor J. Torres[a,g,4]

Edited by Rino Rappuoli, Toscana Life Sciences Foundation, Siena, Italy; received December 23, 2021; accepted May 29, 2022

***Staphylococcus aureus*** **is an opportunistic pathogen and chief among bloodstream-infecting bacteria.** ***S. aureus*** **produces an array of human-specific virulence factors that may contribute to immune suppression. Here, we defined the response of primary human phagocytes following infection with** ***S. aureus*** **using RNA-sequencing (RNA-Seq). We found that the overall transcriptional response to** ***S. aureus*** **was weak both in the number of genes and in the magnitude of response. Using an ex vivo bacteremia model with fresh human blood, we uncovered that infection with** ***S. aureus*** **resulted in the downregulation of genes related to innate immune response and cytokine and chemokine signaling. This muted transcriptional response was conserved across diverse** ***S. aureus*** **clones but absent in blood exposed to heat-killed** ***S. aureus*** **or blood infected with the less virulent staphylococcal species** ***Staphylococcus epidermidis*****. Notably, this signature was also present in patients with** ***S. aureus*** **bacteremia. We identified the master regulator** ***S. aureus*** **exoprotein expression (SaeRS) and the SaeRS-regulated pore-forming toxins as key mediators of the transcriptional suppression. The** ***S. aureus*****–mediated suppression of chemokine and cytokine transcription was reflected by circulating protein levels in the plasma. Wild-type** ***S. aureus*** **elicited a soluble milieu that was restrictive in the recruitment of human neutrophils compared with strains lacking** ***saeRS*****. Thus,** ***S. aureus*** **blunts the inflammatory response resulting in impaired neutrophil recruitment, which could promote the survival of the pathogen during invasive infection.**

bacteremia | immunosuppression | human leukocytes | *Staphylococcus aureus* | MRSA

The human-adapted opportunistic pathogen *Staphylococcus aureus* poses a major public health threat. *S. aureus* causes both community- and hospital-associated infections ranging from skin and soft tissue infections to lethal bloodstream infections (1). The lack of a vaccine against *S. aureus* and its resistance to multiple antibiotics hinder our ability to effectively combat infections. To improve the management of *S. aureus* infections, we must better understand how *S. aureus* manipulates the host immune system.

*S. aureus* pathogenesis depends on a wide array of virulence factors, which target both innate and adaptive immunity (2, 3). These include a variety of toxins and peptides that directly kill leukocytes (4–9). However, many of these virulence factors exhibit exquisite species specificity, affecting human cells but failing to function in mice, the most common animal model used for investigating host responses (3, 10–13). Even virulence factors that can function in mice may still require much higher concentrations (14). Thus, we need to elucidate the impact of *S. aureus* infection to human cells.

During infections, bacteria trigger inflammatory responses, including the secretion of cytokines and chemokines that recruit leukocytes to the area of infection. The recruited neutrophils, monocytes, macrophages, and dendritic cells (DCs) play important roles in both the direct killing of bacteria and the indirect control of infection, such as contributing to the cytokine milieu, clearing debris/damaged cells, and presenting antigen to trigger adaptive immunity. Consistent with this, humans with chronic granulomatous disease as well as other congenital diseases that affect the function of neutrophils and other innate immune cells exhibit an increased risk of Staphylococcal infections (15).

In this study, we discovered that the transcriptional responses of primary human phagocytes—neutrophils, monocytes, macrophages, and DCs—and human whole blood in response to *S. aureus* infection were surprisingly weak. We hypothesized that *S. aureus* actively suppresses cellular responses. Indeed, we identified a signature of suppressed genes that is mediated by virulence factors regulated by the two-component regulator *S. aureus* exoprotein expression (SaeRS). By further examining the cytokine milieu after wild-type (WT) and Δ*sae S. aureus* infection of blood, we show that *S. aureus* downregulates the production of cytokines and chemokines, resulting in decreased recruitment of human neutrophils. Thus, by dampening the responses of human phagocytes, *S. aureus* can protect itself by blunting the recruitment of leukocytes.

## Significance

We show here that infection of human blood with *Staphylococcus aureus* triggers a suppressing transcriptional signature. The signature was conserved across *S. aureus* lineages and present in bacteremic patients infected with *S. aureus*. In contrast to *S. aureus*, we show that *Staphylococcus epidermidis* did not elicit the suppressing signature, implicating *S. aureus* virulence factors as drivers of the suppression. Indeed, the master regulator of virulence, *S. aureus* exoprotein expression (SaeRS), and the SaeRS-regulated toxins were found to be responsible for the "muted" transcriptional response. The *S. aureus*–elicited suppressing response resulted in impaired production of chemokines and decreased recruitment of neutrophils. Thus, we describe a previously unappreciated immunosuppressive strategy employed by *S. aureus* to interfere with the host antimicrobial response.

This article is a PNAS Direct Submission.



[1]E.E.Z., Z.C., and J.C.D. contributed equally to this work.

[2]Present address: Molecular Profiling and Data Science, Regeneron Pharmaceuticals, Inc., Tarrytown, NY 10591.

[3]Present address: Department of Loxo Oncology, Eli Lilly, New York, NY, 10016.

[4]To whom correspondence may be addressed. Email: Kelly.Ruggles@nyulangone.org, png.loke@nih.gov, or Victor.Torres@nyulangone.org.

[5]Present address: Department of Medicine, Section of Genetic Medicine, University of Chicago Pritzker School of Medicine, Chicago, IL 60637.

This article contains supporting information online at http://www.pnas.org/lookup/suppl/doi:10.1073/pnas.2123017119/-/DCSupplemental.

Published July 26, 2022.

## Results

**Methicillin-Resistant *S. aureus* Induces a Muted Cell Type–Specific Leukocyte Transcriptional Response.** To define the transcriptional response of human phagocytes to infection, we performed RNA-Seq on polymorphonuclear neutrophils (PMNs), monocytes, monocyte-derived macrophages (MDMs), and monocyte-derived dendritic cells (MDDCs) from the same three individual donors after infection with the USA300 methicillin-resistant *S. aureus* (MRSA) strain LAC at a multiplicity of infection (MOI) of one (Fig. 1*A*). This low MOI was chosen to avoid overt killing of the cells by *S. aureus* toxins (*SI Appendix*, Fig. S1) (4–8, 16–21). Most of the transcriptional variation among samples was driven by cell type and not infection status (Fig. 1*B*). Response to infection was cell type specific, with little to no overlap in the differentially expressed genes observed among cells types. Interestingly, PMNs responded the most to infection, while monocytes and macrophages responded the least (Fig. 1*C*).

To determine if MRSA infection triggered responses associated with inflammation, uninfected cells were also treated with interferon gamma (IFN-γ) or interleukin 4 (IL-4) to generate transcriptional profiles for comparison. Although MRSA infection resulted in few differentially expressed genes (114 genes with adjusted $P$ value $< 0.05$ and fold change of greater than two across all cell types), the cells responded robustly to treatment with recombinant IFN-γ and IL-4 (Fig. 1*D*–*H*). The overall numbers of differentially expressed genes were greater after cytokine treatment (506 and 554 genes with adjusted $P$ value $< 0.05$ and fold change of greater than two across all cell types for IFN-γ and IL-4, respectively), but also, the magnitude of the overall fold changes was larger (Fig. 1*H*). These data suggest that the phagocytes are capable of responding robustly to stimuli; thus, the infection and not a refractory nature of the isolated cells caused the muted transcriptional changes. In general, MRSA infection of phagocytes affected a variety of signaling and stimuli response pathways (Fig. 1*I*).

**Live MRSA Transcriptionally Suppresses Immune Pathways in Human Whole Blood.** As exposure to live MRSA did not elicit a strong transcriptional response in individual phagocytes, we wondered if an ex vivo model of whole-blood infection that allows for interaction among cell types would facilitate cellular responses. We utilized the TruCulture technology (22), which contains a proprietary culture medium that preserves the physiological state of the leukocytes in the blood for microbial antigen exposure. We infected freshly isolated human whole blood with MRSA at two MOIs (∼0.16 and ∼16). Blood was also exposed to corresponding doses of heat-killed MRSA as heat-killed bacteria have been shown to stimulate whole blood and induce secretion of proinflammatory cytokines (23). Again, we observed that transcriptional variation mainly separated samples based on treatments but not blood donors (Fig. 2*A*). Infection with live MRSA resulted in a suppressed transcriptional signature compared with the corresponding heat-killed MRSA signature (Fig. 2*B*). The suppression was more notable at the higher MOI. Certain genes, such as IL-1β, MIP-1α (CCL3), and MIP-1β (CCL4), were down-regulated by live MRSA but up-regulated by exposure to the corresponding heat-killed MRSA. Parallel pathway analysis of the different conditions revealed that live infection with MRSA down-regulated pathways associated with immune responses, especially cytokine/chemokine signaling, and that the extent of down-regulation increased with the infectious dose (Fig. 2*C*).

**The Transcriptional Repression in Whole Blood Represents a Conserved *S. aureus* Response.** Since the suppressed transcriptional signature observed with live MRSA was initially from a single strain (i.e., strain LAC) and may not be broadly representative, we next cultured blood with a collection of diverse *S. aureus* strains, a strain of the less virulent staphylococcal species *Staphylococcus epidermidis*, and strain LAC that had been heat killed at 95 °C or 65 °C. The lower temperature for heat killing was added in case the previously observed up-regulation of transcripts to heat-killed *S. aureus* could have resulted from exposure to intracellular pathogen-associated molecular patterns (PAMPs) released by high heat. Comparison of differentially expressed genes from the same infectious dose of WT LAC in the initial dataset and this second dataset demonstrated a high degree of concordance (*SI Appendix*, Fig. S2*A*). We observed that transcriptional variation mainly separated *S. epidermidis*–infected and heat-killed *S. aureus*–exposed blood from blood infected with live *S. aureus* strains (Fig. 3*A* and *SI Appendix*, Table S1). The transcriptional response of blood exposed to *S. epidermidis* clustered more tightly with heat-killed MRSA than live *S. aureus* strains, and both the *S. epidermidis* and heat-killed MRSA responses lacked a cluster of down-regulated genes that were notable during infection with live *S. aureus* strains (Fig. 3*B* and *SI Appendix*, Fig. S2*C*).

**SaeRS Mediates Transcriptional Suppression of Immune Responses by *S. aureus*.** As live *S. aureus* strains caused a suppressed transcriptional signature in whole blood, we next sought to identify potential factors involved in the suppression. We infected whole blood with WT LAC and isogenic mutants of LAC lacking an array of virulence factors and master regulators of virulence factors. Transcriptional variation within this isogenic mutant dataset was mainly driven by the difference between live and heat-killed WT LAC. Among the tested mutants, two strains, Δ*sae* (which lacks *saeQRS*) and Δtoxins (which lacks the *hlgABC*, *lukSF-PVL*, *lukAB*, *lukED*, and *hla* genes), shifted noticeably closer to the heat-killed WT LAC (Fig. 3*C*). While the pattern for most differentially expressed genes was similar among WT and mutant strains, k-means clustering identified a cluster of genes (cluster 2) that were down-regulated by the live LAC strains except Δ*sae* and Δtoxins (*SI Appendix*, Fig. S2*B*). This cluster of genes comprised a suppression signature and included IL-1β, MIP-1α, and MIP-1β, which we previously observed to be up-regulated by heat-killed LAC and down-regulated by live LAC. A closer look at the suppression signature cluster showed that Δ*sae* and Δtoxins generated changes in the expression of these genes more similar to heat-killed LAC than to the other live strains (Fig. 3*D*). The SaeRS two-component system is a master regulator of secreted virulence factors, including all the pore-forming toxins that are deleted in the Δtoxins strain (24, 25). While the Δtoxins strain recapitulates much of the transcriptional changes elicited by Δ*sae*, it does not fully replicate the response (Fig. 3*D*). In support of the role for SaeRS, we also observed an absence of the suppression signature in infections with the clinical isolate USA300 ER03928 (Fig. 3*C* and *D*), which was found to harbor a naturally occurring deletion of 11 nucleotides in *saeR* introducing an early stop codon (154 amino acids compared with 228 amino acids in WT).

To determine if Sae-regulated toxins and other factors were causing suppression by inducing increased cell death, leukocytes from buffer-treated, WT-infected, Δ*sae*-infected, and Δtoxins-infected blood were isolated, stained with a fixable viability dye, and analyzed by flow cytometry. As *S. aureus* is a notorious clumper of human blood (26), we used streptokinase to release as many cells as possible. Of note, Δ*sae* does not produce coagulases (25, 27, 28) and thus, does not clump (29, 30), while the WT and Δtoxins strains do. Differences in the percentages of events in the total cell gate are likely attributed to incomplete

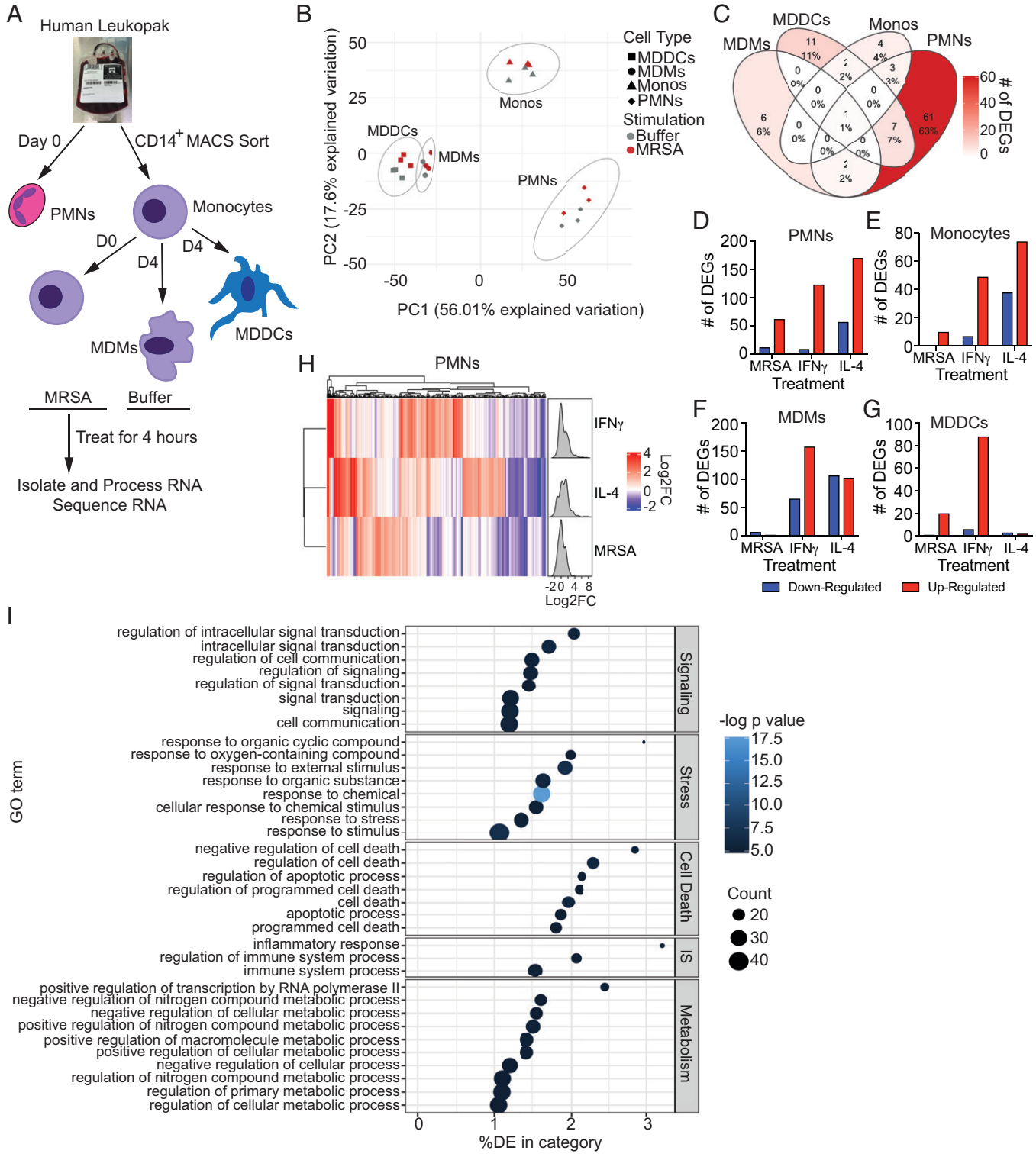


**Fig. 1.** *S. aureus* infection induces a cell type–specific response that is muted compared with cytokine treatment. (*A*) Schematic of the experimental design for RNA-Seq performed with PMNs, CD14$^{+}$ monocytes, MDMs, and MDDCs isolated from the same donors. RNA was isolated 4 h after infection. (*B*) Principal component analysis was performed using the 1,000 most variable genes among all samples. For each sample, principal component 1 (PC1) and principal component 2 (PC2) are plotted. Shapes denote cell type (■, MDDCs; ●, MDMs; ▲, monocytes; ◆, PMNs). Color denotes treatment (gray, buffer; red, *S. aureus* infected). $n = 3$ donors. (*C*) Venn diagram of the number of genes whose transcription was significantly altered by *S. aureus* exposure for the four cell types. Percentages are the percentages of all differentially expressed genes. DEG, differentially expressed gene. (*D*–*G*) Bar graphs of the number of genes that are significantly down-regulated (blue) and up-regulated (red) in comparison with buffer treatment for *S. aureus*–infected, IFN-γ–treated, and IL-4–treated PMNs (*D*), monocytes (*E*), macrophages (*F*), and DCs (*G*). Significantly differentially expressed genes are considered genes with a |log2 fold change (log2FC)| ≥ 1 and an adjusted *P* value ≤ 0.05. (*H*) Heat map of log2FC of genes that are significantly differentially expressed in at least one treatment in PMNs. The histograms show the distribution of log2FCs within each treatment for PMNs. (*I*) Gene ontology (GO) term enrichment analysis of all genes found to be significantly differentially expressed in at least one cell type. Pathways are separated by broad categories. Within each category, pathways are ranked by percentage of differentially expressed genes. Count indicates the number of differentially expressed genes in each GO pathway. IS, immune system; DE, differentially expressed.

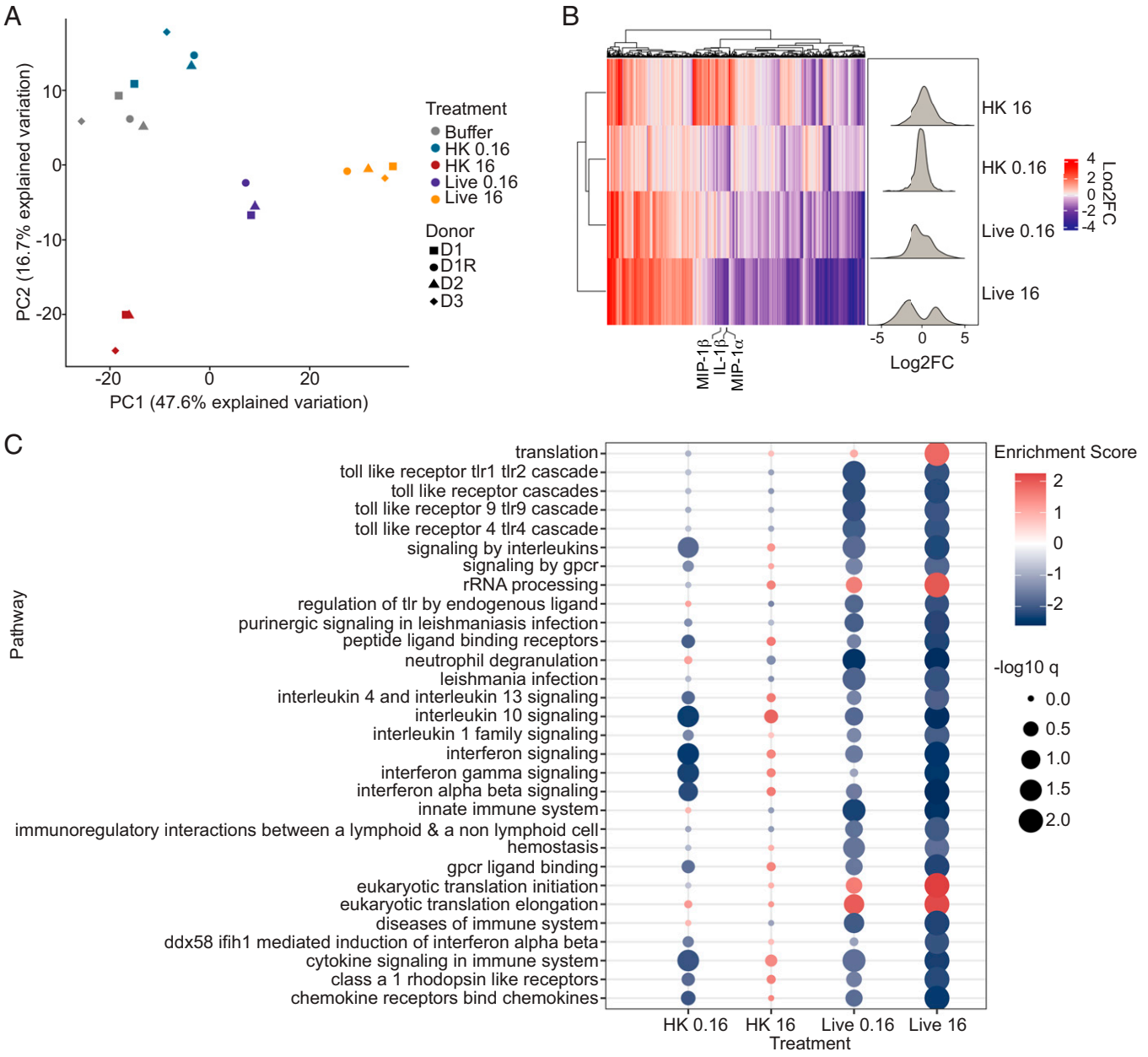


**Fig. 2.** MRSA infection of human whole blood down-regulates genes associated with immune signaling. RNA was isolated 4 h after infection for sequencing. (*A*) Principal component analysis was performed using the 797 genes that are differentially expressed in at least one condition. For each sample, principal component 1 (PC1) and principal component 2 (PC2) are plotted. Shapes denote donor (■, donor 1; ●, donor 1R [second independent infection of donor 1]; ▲, donor 2; ◆, donor 3). Color denotes treatment (gray, buffer; aqua, heat-killed MOI ~ 0.16; red, heat-killed MOI ~ 16; purple, live MOI ~ 0.16; yellow, live MOI ~ 16). MOI designation was determined by the average number of white blood cells per milliliter of blood among donors. (*B*) Heat map of log2 fold change (log2FC) of genes that are significantly differentially expressed in at least one treatment. The histograms show the distribution of log2FCs within each treatment. Significantly differentially expressed genes are considered genes with a $|\log2FC| \geq 1$ and an adjusted $P$ value $\leq 0.05$. (*C*) Parallel pathway analysis (gene set enrichment analysis) was performed. Pathways that were enriched in at least one treatment are graphed in a bubble plot. The color of each bubble indicates the enrichment score. Positive enrichment score (red) indicates the pathway is up-regulated. Negative enrichment score (blue) indicates the pathway is down-regulated. The size of each bubble indicates how statistically strong the enrichment is. rRNA, ribosomal RNA.

disruption of clumping (*SI Appendix*, Fig. S3*A*). The viability of the isolated leukocytes indicated that the infections with the different strains induced similar amounts of cell death (*SI Appendix*, Fig. S3*B*), which suggests that induction of death by Sae-regulated factors is not the only driver of the observed suppression. Collectively, these data implicate toxins as well as other SaeRS-regulated factors in mediating the observed *S. aureus*–suppressive gene signature.

***S. aureus*–Elicited Suppression Signature Is Present in Bacteremic Patients.** Using the suppression signature cluster identified in whole blood and further refined by results with the isogenic mutants, we next asked if this signature is reflected in a meta-analysis of transcriptional data from patients with *S. aureus* bacteremia infections identified in Gene Expression Omnibus (GEO). Transcriptional data of whole blood from bloodstream infection patients (56 patients) and healthy controls from Banchereau et al. (31) and *S. aureus* patients (4 patients) and healthy controls from Hu et al. (32) were analyzed through our pipeline to assess expression of genes in the suppression signature cluster. We compared the patient transcriptional signatures with the suppressed transcriptional signature of live *S. aureus* and *S. epidermidis* (which does not cause a suppressed transcriptional signature). We found that the transcriptional data from patients with bloodstream

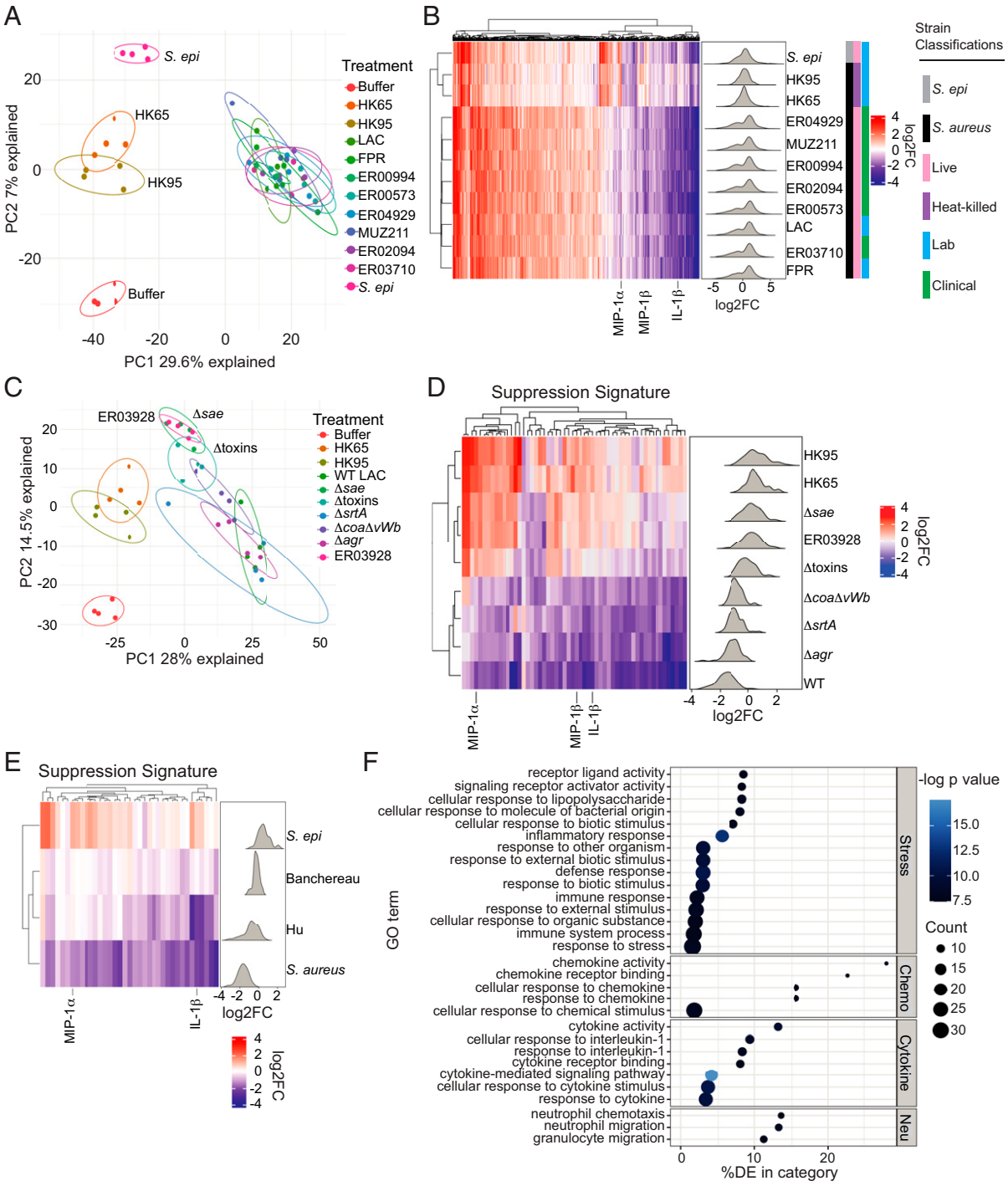


**Fig. 3.** *S. aureus* infection generates an SaeRS-mediated suppression signature in human whole blood. RNA was isolated 4 h after infection for sequencing except for in the Banchereau and Hu cohorts, where blood was isolated from patients. (*A*) Principal component analysis (PCA) was performed on RNA-Seq data where whole blood had been treated with buffer, 65 °C heat-killed *S. aureus* WT LAC, or 95 °C heat-killed *S. aureus* WT LAC or infected with WT LAC (CC8), FPR (CC8), ER00994 (CC8), ER00573 (CC8), ER04929 (CC8), MUZ211 (CC30), ER02094 (CC5), ER03710 (CC8), and *S. epidermidis* (*S. epi*). For each sample, principal component 1 (PC1) and principal component 2 (PC2) are plotted. Color denotes treatment. Infection with all strains was performed at an MOI of ~16. $n = 4$. (*B*) Heat map of log2 fold change (log2FC) of genes that are significantly differentially expressed in at least one treatment of the indicated clinical and laboratory strains (*S. epi*, LAC, and FPR). Significantly differentially expressed genes are considered genes with a $|\log2FC| \geq 1$ and an adjusted $P$ value $\leq 0.05$. The histograms show the distribution of log2FC within each treatment. (*C*) PCA was performed on RNA-Seq data where whole blood from four human donors had been exposed to buffer, 65 °C heat-killed *S. aureus* WT LAC, 95 °C heat-killed *S. aureus* WT LAC, live WT LAC, isogenic mutants of LAC for Δ*sae*, the leukocidins (Δtoxins), Sortase A (Δ*srtA*), the clumping factors coagulase and von Willebrand factor binding protein (Δ*coa*Δ*vWb*), and Δ*agr*. For each sample, PC1 and PC2 are plotted. Color denotes treatment. Infection with all strains was performed at an MOI of ~16. $n = 4$. (*D*) Heat map of log2FC of only the suppression signature cluster genes for indicated strains. The histograms show the distribution of log2FC within each treatment. (*E*) Expression data from cohorts of *S. aureus*–infected patients (i.e., Banchereau and Hu) were identified in GEO and processed using our pipeline. Fold change for the clinical data is expression in infection compared with healthy controls. Heat map of log2FC of only the genes identified in the suppression signature cluster for clinical cohorts, *S. epi*, and average *S. aureus* ex vivo response from *SI Appendix*, Fig. S2*B*. The histograms show the distribution of log2FC within each treatment. (*F*) Gene ontology (GO) analysis was performed for the genes identified in the suppression signature. Pathways associated with the genes are shown. The size of the bubble indicates the number of genes in the pathways. The color of the bubble shows the statistical significance of the pathway's association with suppression signature genes. Pathways are separated by broad categories. Within each category, pathways are ranked by the percentage of differentially expressed genes. Chemo, chemokines; Neu, neutrophils; DE, differentially expressed.

infections clustered with the *S. aureus* signature rather than the *S. epidermidis* signature (Fig. 3*E*). Thus, the suppressed transcriptional signature identified in the ex vivo bacteremia model is also observed in the blood of patients with *S. aureus* bacteremia.

**_S. aureus_ Blunts the Production of Cytokines and Chemokines.** As the genes identified in the suppression signature cluster seem to represent a conserved *S. aureus* signature that is present both ex vivo and in patients, we next performed gene ontology analysis to determine which pathways are affected in this cluster (Fig. 3*F*). Many of the pathways identified were associated with cytokine and chemokine signaling, including pathways such as neutrophil chemotaxis and granulocyte migration. Interestingly, MIP-1α and MIP-1β, which are directly involved in monocyte migration (33), and IL-1β, whose signaling induces secretion of the chemokine IL-8 (34), are members of the suppression signature cluster.

We next determined if the transcriptional suppression of cytokine and chemokine expression by *S. aureus* resulted in changes in the production and secretion of these soluble mediators. Exposure of whole blood with heat-killed LAC induced the production of copious levels of proinflammatory cytokines and chemokines (e.g., IL-8, MIG, MIP-1α, MIP-1β, TNFα, and IL-1β) compared with infection with live WT LAC (Fig. 4*A* and *SI Appendix*, Fig. S4). Comparison of cytokine/chemokine profiles in the blood after exposure to WT LAC, Δtoxins, and Δ*sae* showed significant reduction of IL-8, MIP-1α, and TNFα in an SaeRS- and toxin-dependent manner, while MIP-1β, IL-1α, IL-1β, and IL-6 were decreased in an SaeRS-dependent manner (Fig. 4*B* and *SI Appendix*, Fig. S5). Consistent with our data, TNFα has previously been shown to be produced in higher amounts by *saeRS* mutants than WT after 3 h of infection of whole blood (35). While IL-1β belongs to the transcriptional suppression signature cluster, IL-1β protein requires processing in order to be secreted (36); thus, we see higher IL-1β secretion in WT *S. aureus* infection than buffer treatment. Comparison among the broad collection of clonal complex 8 (CC8) strains with CC5 and CC30 strains also showed a significantly greater induction of IL-8, MIG, MIP-1α, and TNFα by ER03928 and *S. epidermidis* compared with the other strains (Fig. 4*C* and *SI Appendix*, Fig. S6).

To confirm that the suppression signature is specific for *S. aureus* and not *S. epidermidis*, we examined levels of IL-8, MIP-1α, and TNFα after infection with four additional *S. epidermidis* strains and *S. aureus* strains representing eight clonal complexes and observed a consistent suppressive response by the *S. aureus* strains compared with the *S. epidermidis* strains (*SI Appendix*, Fig. S7). As previously observed, the Δ*sae* strain showed a response similar to the *S. epidermidis* strains (*SI Appendix*, Fig. S7). These data further support the observation that the suppression phenotype represents a broad *S. aureus* feature.

To test whether *S. aureus* infection actively suppresses the immune response, whole blood was initially infected for 2 h with WT or Δ*sae S. aureus* (strain LAC) or exposed to buffer, at which point the blood was exposed to either heat-killed WT *S. aureus* or buffer for an additional 2 h. The difference in cytokine concentration between 4 and 2 h postinitial infection was determined (*SI Appendix*, Fig. S8*A*). At 2 h postinfection, WT-infected blood already exhibited a blunted production of cytokines compared with Δ*sae*-infected blood for all cytokines tested except IL-1β (*SI Appendix*, Fig. S8*B*). Comparison of cell viability between leukocytes isolated from WT-infected blood and Δ*sae*-infected blood at 2 h postinfection determined that the amount of cell death in whole blood was similar between the infections (*SI Appendix*, Fig. S8*C*). Supporting the idea that this is an active process, exposure to heat-killed bacteria greatly increased the levels of cytokines in whole blood originally exposed to buffer but not whole blood previously infected with WT *S. aureus* (*SI Appendix*, Fig. S8*D*). As Δ*sae* infection seems to max out cytokine levels, heat-killed exposure of whole blood previously infected with Δ*sae* did not further increase the concentration of cytokine in the blood compared with buffer exposure (*SI Appendix*, Fig. S8*D*). The similarity in cell viability between WT- and Δ*sae*-infected blood further suggests that the suppression witnessed in WT-infected blood upon exposure to heat-killed bacteria is not the consequence of changes in cell viability. Hence, SaeRS-regulated virulence factors, including toxins, mediate active suppression of cytokine and chemokine production during *S. aureus* infection.

**_S. aureus_–Dampened Chemokine Response Results in Impaired Neutrophil Migration.** While TNFα, IL-6, IL-1α, and IL-1β induce antimicrobial functions, IL-8, MIG, MIP-1α, and MIP-1β are all chemokines important for the recruitment of innate and adaptive immune cells to the site of infection (33, 37–42). Suppression of these chemokines by *S. aureus* could potentially affect the recruitment of phagocytes to the infected area. As PMNs play an important role in the clearance of *S. aureus*, inhibiting their recruitment to the site of infection could enhance the probability of infection. While IL-8 is an important chemokine for neutrophil recruitment (38), the overall milieu generated by WT *S. aureus* infection could potentially compensate for the decrease in IL-8 levels from WT infection compared with Δ*sae* infection. We performed neutrophil migration assays with primary human PMNs from 12 healthy human donors using a modified Boyden chamber to measure differences in migration to plasma from WT LAC infection, Δ*sae* LAC infection, and buffer treatment. While plasma from WT infection triggered higher neutrophil recruitment than control plasma (buffer-treated blood), plasma from Δ*sae*-infected blood was more chemotactic than the plasma from WT LAC-infected blood (Fig. 4*D*). The area under the curve (AUC) serves as a proxy for the amount of migration, while the slope of the linear portion shows the rate of migration. For both AUC and slope, we calculated the fold change of migration toward plasma from both WT infection and Δ*sae* infection compared to migration toward plasma from buffer-treated blood. We observed that WT LAC reduced the amount and rate of neutrophil migration compared with infections with Δ*sae* LAC (Fig. 4*E* and *F*). Altogether, these data support the hypothesis that *S. aureus* inhibits the host chemokine response to diminish the recruitment of PMNs in an SaeRS-dependent manner.

## Discussion

In this study, we show that primary human phagocytes mount transcriptional responses that are surprisingly weak in response to *S. aureus* infection. To determine if *S. aureus* was actively suppressing host responses, we implemented an ex vivo bacteremia model where freshly isolated human blood was cultured with live or heat-killed MRSA. These studies exposed a suppressing transcriptional signature that was observed in live infections and not by exposure of blood to heat-killed *S. aureus* or to *S. epidermidis*. By examining the host expression profile elicited by isogenic *S. aureus* mutants and clinical strains, we identified the two-component virulence regulator SaeRS and the SaeRS-regulated toxins as key mediators of the observed

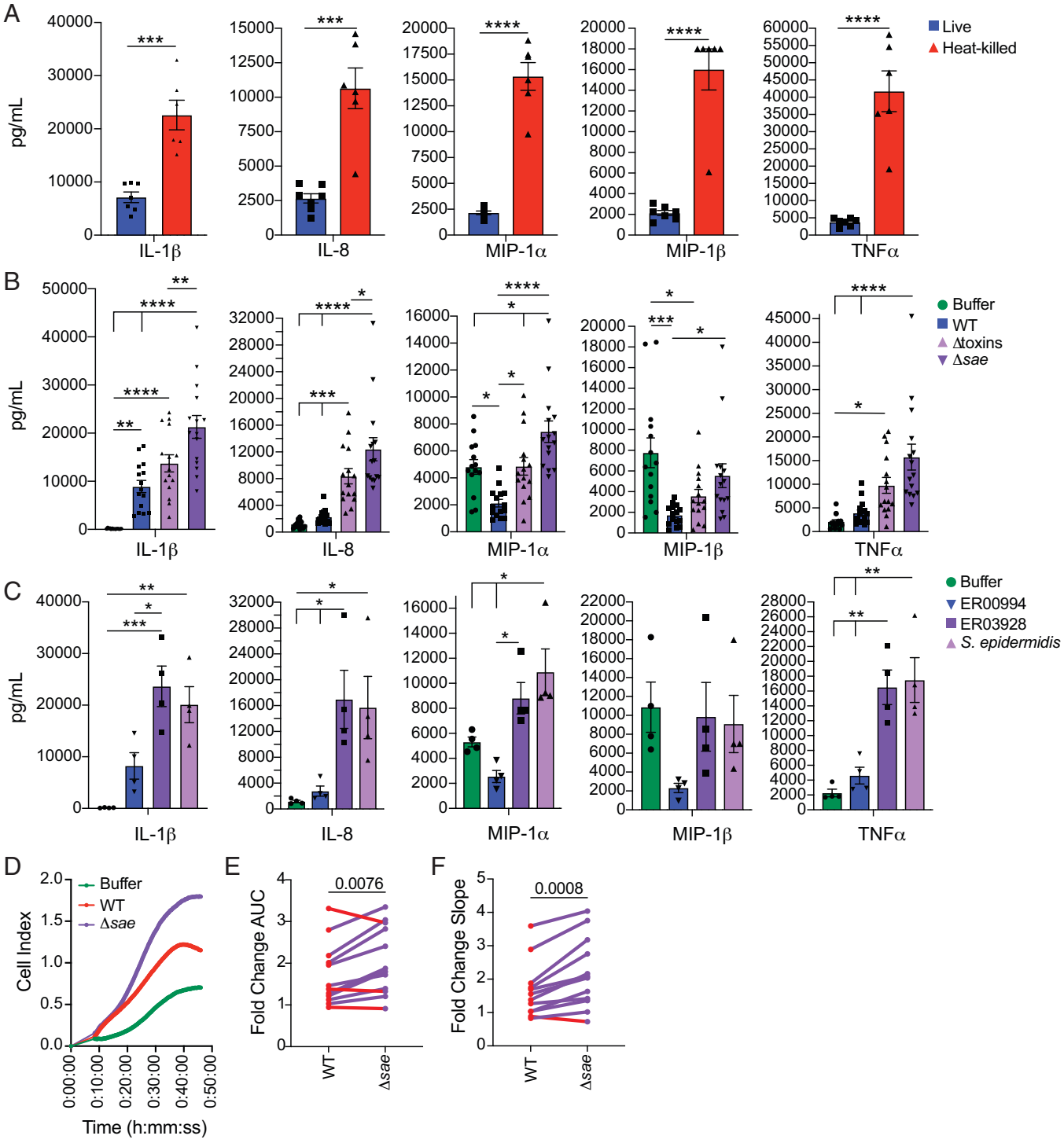


**Fig. 4.** *S. aureus* infection reduces chemokine and cytokine secretion in human whole blood and dampens neutrophil recruitment. Sera used for cytokine profiling in *A*–*C* and neutrophil migration assays were collected from whole blood 4 h after infection. (*A*) Concentration of cytokines/chemokines per milliliter of blood was quantified by the magnetic bead assay for blood infected with live *S. aureus* (blue; $n = 7$) at an MOI of ∼16 or treated with heat-killed *S. aureus* (red; $n = 6$). Error bars represent SEM. Student's *t* tests were performed to determine significance. ***$P < 0.001$; ****$P < 0.0001$. (*B*) Concentration of cytokines/chemokines per milliliter of blood was quantified by the magnetic bead assay for blood infected with WT LAC (blue; $n = 15$), LAC Δtoxins (lilac; $n = 15$), or LAC Δ*sae* (purple; $n = 15$) at an MOI of ∼16 or treated with buffer (green; $n = 14$). Error bars represent SEM. One-way ANOVAs with Tukey's multiple comparisons tests were performed to determine significance. *$P < 0.05$; **$P < 0.01$; ***$P < 0.001$; ****$P < 0.0001$. (*C*) Concentration of cytokines/chemokines per milliliter of blood was quantified by the magnetic bead assay for blood infected with USA300 strain ER00994 (blue; $n = 4$), USA300 strain ER03928 (purple; $n = 4$), or *S. epidermidis* (lilac; $n = 4$) at an MOI of ∼16 or treated with buffer (green; $n = 4$). Error bars represent SEM. One-way ANOVAs with Tukey's multiple comparisons tests were performed to determine significance. *$P < 0.05$; **$P < 0.01$; ***$P < 0.001$. (*D*) Representative graph of migration of a single neutrophil donor exposed to supernatants from buffer, WT, and Δ*sae*-treated blood. (*E*) Graph of the fold change of the AUC compared with buffer. Each dot represents a single neutrophil donor. $n = 12$. Lines connect the same donor exposed to supernatants from WT and Δ*sae* infection. Paired Student's *t* test was performed. (*F*) Graph of the fold change of the slope of the linear portion compared with buffer. Each dot represents a single neutrophil donor. $n = 12$. Lines connect the same donor exposed to supernatants from WT and Δ*sae* infection. Paired Student's *t* test was performed.

suppressing transcriptional signature. Importantly, the suppressing transcriptional signature was also observed in patients with *S. aureus* bacteremia. By performing cytokine analyses and PMNs migration assays, we discovered that during *S. aureus* infection, Sae-regulated virulence factors actively down-regulate the production of chemokines, which blunt the recruitment of PMNs. Thus, we described herein a strategy where *S. aureus* blunts the production of cytokines and chemokines to prevent the full recruitment of pathogen-killing phagocytes.

Previously, a transcriptional profile study was performed where PMNs were infected with *S. aureus* at an MOI of 10 (43). This study revealed a more active transcriptional response compared with the current study that used an MOI of one. The different models may represent different infection dynamics and suggest that phagocytes respond differently depending on the context of infection. To validate our findings in a more physiological setting, we employed an ex vivo bacteremia model of infection. We discovered that while heat-killed *S. aureus* induces a robust proinflammatory response in whole blood (Fig. 2) as seen previously (23), infection with live *S. aureus* actively suppressed genes related to chemokine and cytokine signaling (Figs. 2–4). Heat-killed bacteria or purified PAMPs used to interrogate the response of whole blood to infection can activate receptors that recognize bacterial products and the downstream consequences of recognition (23, 44–46). However, heat-killed bacteria may have inactivated virulence factors, whereas live bacteria undergo regulation and processes that are informed by the environment, including whole blood and blood products (47). The suppression signature that we described here seems to be a consequence unique to live bacteria, which can perform activities and generate virulence products that influence the immune response. The dependence of the suppression signature on the virulence factors regulated by Sae in live bacteria highlights the thin line that can exist between circumventing and activating immune responses. In other model systems, live bacteria generate a stronger proinflammatory response than heat-killed bacteria through the recognition of vitaPAMPs, such as cyclic-di-adenosine mono-phosphate (c-di-AMP), which require bacteria to be alive upon phagocytosis (48, 49). Hence, the context of the host–pathogen interaction matters, and the complexity of competing signals generated during infection necessitates different experimental models to understand different aspects of infection. Remarkably, the suppression signature described here was also detected in blood isolated from *S. aureus* bacteremic patients from two independent cohorts (Fig. 3) (31, 32), indicating that it is not an artifact of our ex vivo model.

Sensing and responding to the environment are essential to the survival of bacteria and the establishment of infection. Two-component systems, such as SaeRS, integrate environmental signals into an appropriate bacterial response (50). Many of the known SaeRS activation signals, such as human neutrophil peptides 1 to 3, calprotectin, and high concentrations of hydrogen peroxide (51, 52), reflect the presence of PMNs. As PMNs are critical for controlling *S. aureus* infection (17), detecting the presence of these cells and adjusting the virulence output should help *S. aureus* circumvent PMNs. The cytokine milieu from infection with WT *S. aureus* leads to a dampened migration of PMNs compared with the cytokine milieu from infection with an isogenic *sae* mutant (Fig. 4*D*–*F*). During infection, the dampening of the cytokine/chemokine response mediated by SaeRS-regulated virulence factors could protect *S. aureus* by both limiting the number of immune cells recruited to the site of infection and impairing the ability of immune cells present to directly kill the bacteria.

The SaeRS system is a master regulator of secreted virulence factors, including pore-forming toxins, coagulase, superantigen-like proteins, and proteases (25, 53, 54). Interestingly, the virulence factors under the control of SaeRS in *S. aureus* are not found in *S. epidermidis* (54). The lack of these virulence factors likely explains why we do not observe the suppression signature during *S. epidermidis* infection (Fig. 3 and *SI Appendix*, Fig. S7). Herein, we found that an isogenic strain lacking all the β-barrel pore-forming toxins (i.e., *lukAB*, *hlgACB*, *lukED*, *lukSF-PV*, and α-toxin) relieved most of the suppression observed by *S. aureus* infection but did not fully recapitulate the relief measured during infection with the Δ*sae* strain (Fig. 3). As the SaeRS system is known to directly regulate ∼20 virulence factors (27, 28, 55), the observed suppression in whole blood may result from a cumulative effect of these virulence factors. As we know that toxins play a role in generating the observed suppression signature, it seems unlikely that a single SaeRS-controlled factor would be responsible for the observed phenotype. Further experiments to determine the upstream mechanism of suppression are required. It is possible that toxins and other virulence factors disrupt signaling through receptors needed to activate transcription through competition for the receptors, destruction of the host ligand or receptor, or enhancing recycling of the receptors off the cell surface. The potential cooperative effects among SaeRS-regulated virulence factors are an important avenue of research that deserves further consideration.

The manipulation and subversion of the host immune response by pathogens impair the ability of the host to effectively clear serious infections. With its multifaceted arsenal of virulence factors that target multiple arms of the immune system, *S. aureus* provides a prime example of pathogens that continue to pose serious public health threats, causing a wide variety of diseases. *S. aureus* is one of the most common infections in people, in particular people suffering from congenital diseases affecting neutrophils (15), demonstrating the importance of neutrophils in combating *S. aureus*. We identified here a suppressed transcriptional signature conserved across *S. aureus* strains that results in decreased production of cytokines and chemokines, which in turn, dampens the recruitment of neutrophils. Further understanding of how *S. aureus* modulates virulence in different types of infection to influence or circumvent the host response to infection is crucial for the development of effective therapeutics to treat and prevent *S. aureus* infections.

## Materials and Methods

**Ethics Statement.** The study protocol to recruit, consent, and enroll healthy subjects as donors of whole blood was reviewed and approved by the New York University Langone Health Institutional Review Board (protocol no. i14-02129_CR6). LeukoPaks were obtained from anonymous blood donors with informed consent from the New York Blood Center.

**Bacterial Strains and Culture Conditions.** The *S. aureus* isolates used in this study are listed in *SI Appendix*, Table S1. *S. aureus* USA300 strain AH-LAC (56) was used in all experiments as the WT USA300 MRSA strain unless otherwise indicated. Bacteria were routinely grown at 37 °C on tryptic soy agar. Overnight cultures were grown in 5 mL tryptic soy broth (TSB) in 15-mL tubes under shaking conditions at 180 rpm with a 45° angle. A 1:100 dilution of overnight culture was subcultured into TSB and incubated for another 3 h. For individual phagocyte infections, bacteria were resuspended in Roswell Park Memorial Institute Medium (RPMI) + 10 mM 4-(2-hydroxyethyl)-1-piperazineethanesulfonic acid (HEPES) + 0.05% human sera albumin (HSA; Seracare). Optical Density 600 nanometer (OD600) readings were taken, and bacteria were normalized to $\sim 5 \times 10^8$/mL. Bacteria were opsonized by incubation of 20% normal human serum, prepared as previously described (57), for 30 min at 37 °C under shaking conditions. Bacteria were washed, resuspended in RPMI + 10% fetal bovine serum (FBS), and diluted to $1 \times 10^7$/mL. For whole-blood infections, bacteria

were washed and resuspended in RPMI + 10% FBS. OD600 readings were taken, and bacteria were normalized to $\sim 5 \times 10^8$/mL. For MOI 0.16, bacteria were diluted 100-fold. Appropriately diluted bacteria for each MOI were heat killed for 30 min at either 95 °C or 65 °C.

**Cell Isolation and Differentiation Protocol.** Primary human PMNs and peripheral blood mononuclear cells (PBMCs) were isolated by Ficoll gradient separation as previously described (58). $CD14^+$ monocytes were then isolated from the PBMC fraction by positive selection. In brief, PBMCs were resuspended in MACS® buffer (phosphate buffered saline (PBS) + 0.05% bovine serum albumin (BSA) + 2 mM ethylenediaminetetraacetic acid (EDTA)) at a concentration of $1 \times 10^8$ PBMCs per 950 μL. Fifty microliters of $CD14^+$ microbeads (Miltenyi Biotec) were added for every $1 \times 10^8$ PBMCs. Cells were incubated for 20 min at 4 °C, washed, and filtered through a cell strainer. The cells were run on an AutoMACS Pro (Miltenyi Biotec) using the "Posselds" program. Monocytes were used directly after sorting. MDDCs and MDMs were differentiated from $CD14^+$ monocytes by culturing the cells for 4 d at 37 °C and 5% $CO_2$ in RPMI medium supplemented with 10% FBS, 10 mM HEPES, 100 U/mL penicillin, and 100 μg/mL streptomycin with either 110 U/mL granulocyte-macrophage colony-stimulating factor (GM-CSF) (Leukine; Sanofi) and 282 U/mL IL-4 (Affymetrix; eBioscience) for DCs or 280 U/mL GM-CSF for macrophages. Media were replenished with fresh cytokine on day 2. PMNs, monocytes, DCs, and macrophages were confirmed by flow cytometry by staining with anti-CD14–fluorescein isothiocyanate (FITC) mAb, anti-CD11c–peridinin chlorophyll protein-Cyanine5.5 (PerCPcy5.5) mAb, and anti–human leukocyte antigen DR isotype (HLA-DR)–allophycocyanin Cyanine7 mAb (BioLegend). After washing, samples were fixed with PBS supplemented with 2% FBS, 2% paraformaldehyde, and 0.05% sodium azide and analyzed by flow cytometry (Cytoflex; Beckman Coulter). Data were analyzed using FlowJo software.

**Phagocyte Infection Protocol.** Isolated PMNs and monocytes and differentiated DCs and macrophages were resuspended in clear RPMI 1640 + 10% FBS. A total of $1 \times 10^5$ cells were added to each well. Bacteria was added at an MOI of one. For cytokine stimulation, 10 ng/mL of IFN-γ (carrier free; R&D Systems) and 1,000 IU/mL (78.125 ng/mL) IL-4 (carrier free; Life Technologies) were added to the appropriate well. Plates were spun for 5 min at 1,200 rpm and incubated for 4 h at 37 °C and 5% $CO_2$. Cells were then washed with PBS. Cells were resuspended in RLT buffer (Qiagen) and vortexed for 1 min before being placed at −80 °C. RNA for each donor was then isolated with the RNeasy Plus Mini Kit (Qiagen) following the protocol with on-column DNase Digestion (Qiagen).

**Whole-Blood Infection Protocol.** Blood was drawn from healthy human donors according to our institutional review board protocol. A portion of the blood was run for complete blood count (Beckman Coulter). One milliliter of blood per tube was then added to TruCulture tubes and inverted gently to mix. Stimulations were added to appropriate tubes at the following final concentrations: buffer (RPMI + 0.6% FBS), live *S. aureus* ($10^8$/mL of blood, MOI 16 and $10^6$/mL of blood, MOI 0.16), and heat-killed *S. aureus* ($10^8$/mL of blood, MOI 16 and $10^6$/mL of blood, MOI 0.16). Tubes were inverted gently to mix. Tubes were incubated for 4 h at 37 °C with gentle rotation. Tubes were spun for 10 min at $450 \times g$ without break. For RNA-Seq, supernatants were removed, and a small portion was frozen for cytokine analysis. The pellets were resuspended in 2 mL of PAXGene reagent. Tubes were incubated at room temperature for 2 h and placed at 4 °C overnight. RNA was then isolated using the PAXGene protocol. For migration experiments, supernatants were collected and syringe filtered with a 0.2-μm filter. Aliquots were frozen and stored at −80 °C for both cytokine analysis and use in migration assays. For flow cytometry after 2 or 4 h of infection, supernatants were removed, and cells were used for staining.

For heat-killed restimulation experiments, blood was initially infected with live *S. aureus* ($10^8$/mL of blood, MOI 16) or buffer for 2 h. A 200-μL aliquot was removed to collect serum for cytokines. Either buffer or heat-killed *S. aureus* ($10^8$/mL of blood, MOI 16) was added for an additional 2 h before being spun down, and serum was collected.

**Gene Expression Analysis.** Libraries were generated for each donor using the CelSeq2 protocol (59) and were sequenced on Illumina HiSeq (phagocyte infection) and Illumina NovaSeq (whole blood). The gene expression data are deposited in GEO.

Reads were mapped by Bowtie2.3.1 (60) to the hg38 reference genome, and uniquely mapped indices were determined by HTSeq-counts (61). Differential expression analysis was performed in R (v3.5.1) using DESeq2 (62). The significant differentially expressed genes were determined with the cutoff of log2 fold change $> 1$ or $< -1$ and adjusted $P$ value $< 0.05$ compared with buffer controls. The pathway analysis was performed by using R package goseq (63).

The suppressive signature gene set was determined by using the method of k-means clustering. The input matrix is the log2 fold change of heat-killed 65, heat-killed 95, Δ*sae*, Δ*srtA*, Δ*agr*, Δ*coa*, Δtoxins, and WT *S. aureus*. The elbow plot indicated that the optimal number was five. The cluster where genes are up-regulated in the heat-killing process and down-regulated in WT was identified as the suppressive signature.

Clinical cohort data were obtained from Hu et al. (32) and Banchereau et al. (31). Clinical cohort analysis was performed via R package limma (64). Fold change is the expression in infected patients compared with healthy controls. Differentially expressed probes were determined with the cutoff log2 fold change $> 1$ or log2 fold change $< -1$ and adjusted $P$ value (padj) $< 0.05$.

Visualization was performed by using R packages ggplot2 (65), ComplexHeatmap (66), and ggVennDiagram (67).

**Cytokine Profiling.** Cytokine profiles were determined using the MILLIPLEX MAP Human Cytokine/Chemokine/Growth Factor Panel A 48 PLEX Magnetic Bead Panel kit (Millipore Sigma). In brief, premixed magnetic beads that bind specific cytokines were added to wells containing supernatant from whole-blood infections, standards, background, and quality control. The plate was incubated with shaking at room temperature for 2 h. The plate was washed on a magnet. Detection antibody was added to each well and incubated with shaking at room temperature for 1 h before adding streptavidin-phycoerythrin to each well and incubating for an additional 30 min. The plate was washed on a magnet. The wells were resuspended in drive fluid and run on MAGPIX with xPONENT software. Calculation of concentration per milliliter of supernatant was performed by the software. Data were exported from software. To determine the concentration of cytokine per milliliter of blood, the concentration was multiplied by three. Data were imported to Prism9. Statistical analyses were performed in Prism for each individual cytokine. For comparison of three or more samples, a one-way ANOVA with Tukey's multiple comparisons test was performed to determine significance. For comparison of two samples, a Student's $t$ test was performed.

**Chemotaxis Assay.** Chemotaxis assays were carried out with CIM-16 well plates and an xCELLigence RTCA-DP instrument (Roche Diagnostics) with modifications from previous descriptions (68). The undersides of the membrane where the microelectrodes are located were coated with 50 μL of 50 μg/mL fibronectin in PBS per well overnight at 4 °C. The following day, the membranes were washed three times with PBS. Filtered supernatants from whole blood treated with buffer or infected with WT or Δ*sae* strains were warmed to 37 °C and loaded into the lower chamber (160 μL volume). Following attachment of the upper chamber, 35 μL of prewarmed RPMI + 0.05% HSA was added to each well. The plate was placed in the RTCA-DP machine and allowed to equilibrate for 60 min. During this time, freshly isolated PMNs were resuspended in RPMI + 0.05% HSA at a concentration of $1.2 \times 10^7$/mL. A background reading was taken for each plate; 100 μL of neutrophils were quickly added to each well. Data were collected every 10 s over the course of 2 h (721 sweeps). Data points were exported and graphed in Prism9. Prism was used to determine the AUC and the slope of the linear portion of the graph. Fold change compared with supernatants from buffer-treated blood was calculated for each neutrophil donor for AUC and slope of each infection. Statistical significance was determined in Prism using the paired Student's $t$ test.

**Flow Cytometry.** Cell pellets were resuspended in 2% FBS–PBS and incubated with streptokinase for 10 min shaking at 37 °C; 100 μL were removed, washed with PBS, and resuspended in 1:100 fixable viability dye efluor450 (eBioscience) in PBS. Cells were incubated at 4 °C for 30 min protected from light. Cells were washed two times with 2% FBS–PBS. Red blood cells were then lysed, and the sample was fixed with one-step fix/lyse solution (eBioscience) following the protocol. Cells were run on a CytoFlex analyzer (Beckman Coulter). Analysis was performed using FlowJo software v10.

**RNA-Seq Data.** Gene expression data from myeloid cells and whole blood exposed to *S. aureus* have been deposited in GEO under accession number

GSE193219. The cytokine profile studies are publicly available (accession no. GSE131990). Clinical cohort data were obtained from publicly available studies (accession nos. GSE40396 and GSE30119).

**Data Availability.** Gene expression data from myeloid cells and whole blood exposed to *S. aureus* have been deposited in GEO (accession no. GSE193219) (69). The cytokine profile studies are available in GEO (accession no. GSE131990) (70). Clinical cohort data were obtained from GEO (accession nos. GSE40396 and GSE30119) (71, 72).

**ACKNOWLEDGMENTS.** We thank members of the laboratory of V.J.T. for helpful discussions over the years and the whole-blood donors and the phlebotomists for making the study possible. Special thanks to Dr. Evelien Berends and Dr. Mei San Tang for help starting the project; Amber Cornelius and the New York University (NYU) Langone Health Vaccine Center for running complete blood count on the blood samples; Dr. Alex Horswill (University of Colorado Anschutz School of Medicine) for providing the Δ*coa*Δ*vWb* strain; Dr. Harm Van Bakel (Icahn School of Medicine at Mt. Sinai) for providing clinical bloodstream isolates (ER04929, ER00994, ER02094, ER00573, ER03710, and ER03928); Dr. Bo Shopsin and Dr. Magdalena Podkowik (NYU) for providing the CC22, CC45, and CC5 502A *S. aureus* isolates; and Dr. Ken Caldwell (NYU) for commenting on the manuscript. We acknowledge help from the NYU Langone's Genome Technology Center for performing all the RNA sequencing. E.E.Z. was supported in part by National Institute of Allergy and Infectious Diseases (NIAID)–Supported Institutional Research Training Grant on Infectious Disease & Basic Microbiological Mechanisms T32 AI007180. J.C.D. was supported in part by NIAID-Supported Institutional Research Training Grant in Immunology and Inflammation T32 AI100853. A.W. was supported by National Heart, Lung, & Blood Institute Award K99 HL151963. K.A.L. was supported by Cystic Fibrosis Postdoctoral Research Fellowship Award LACEY19FO. This research was also supported in part by the Intramural Research Program of the NIAID, NIH (P.L.). Research in the laboratory of V.J.T. is supported by NIH, NIAID Awards AI099394, AI105129, AI121244, AI137336, AI140754, and AI133977. V.J.T. is a Burroughs Wellcome Fund Investigator in the Pathogenesis of Infectious Diseases. The NYU Langone Health Genome Technology Center and the Cytometry and Cell Sorting Laboratory are shared resources partially supported by Laura and Isaac Perlmutter Cancer Center Support Grant P30CA016087 from National Institutes of Health The National Cancer Institute (NIH-NCI).

Author affiliations: [a]Department of Microbiology, New York University Grossman School of Medicine, New York, NY 10016; [b]Institute for Systems Genetics, New York University Grossman School of Medicine, New York, NY 10016; [c]Department of Medicine Cardiology, New York University Grossman School of Medicine, New York, NY 10016; [d]Department for Biochemistry and Molecular Pharmacology, New York University Grossman School of Medicine, New York, NY 10016; [e]Division of Translational Medicine, Department of Medicine, New York University Grossman School of Medicine, New York, NY 10016; [f]Laboratory of Parasitic Diseases, National Institute of Allergy and Infectious Diseases, NIH, Bethesda, MD 20892; and [g]Antimicrobial-Resistant Pathogens Program, New York University Grossman School of Medicine, New York, NY 10016

Author contributions: E.E.Z., K.V.R., P.L., and V.J.T. designed research; E.E.Z., X.Z., A.W., and K.A.L. performed research; E.A.F. and D.F. contributed new reagents/analytic tools; E.E.Z., Z.C., J.C.D., Z.L., and K.V.R. analyzed data; E.A.F., D.F., and P.L. contributed mentoring, resources, and know-how; K.V.R. contributed mentoring and know-how; V.J.T. contributed mentoring and resources; and E.E.Z., P.L., and V.J.T. wrote the paper.

Competing interest statement: V.J.T. has consulted for Janssen Research & Development, LLC and has received honoraria from Genentech and Medimmune. V.J.T. is also an inventor on patents and patent applications filed by New York University, which are currently under commercial license to Janssen Biotech Inc. Janssen Biotech Inc. provides research funding and other payments associated with a licensing agreement.

1. S. Y. Tong, J. S. Davis, E. Eichenberger, T. L. Holland, V. G. Fowler Jr., *Staphylococcus aureus* infections: Epidemiology, pathophysiology, clinical manifestations, and management. *Clin. Microbiol. Rev.* **28**, 603–661 (2015).
2. V. Thammavongsa, H. K. Kim, D. Missiakas, O. Schneewind, Staphylococcal manipulation of host immune responses. *Nat. Rev. Microbiol.* **13**, 529–543 (2015).
3. A. N. Spaan, J. A. G. van Strijp, V. J. Torres, Leukocidins: Staphylococcal bi-component pore-forming toxins find their receptors. *Nat. Rev. Microbiol.* **15**, 435–447 (2017).
4. A. L. Dumont *et al.*, Characterization of a new cytotoxin that contributes to *Staphylococcus aureus* pathogenesis. *Mol. Microbiol.* **79**, 814–825 (2011).
5. H. B. Fackrell, G. M. Wiseman, Properties of the gamma haemolysin of *Staphylococcus aureus* 'Smith 5R'. *J. Gen. Microbiol.* **92**, 11–24 (1976).
6. A. Gravet *et al.*, Characterization of a novel structural member, LukE-LukD, of the bi-component staphylococcal leucotoxins family. *FEBS Lett.* **436**, 202–208 (1998). Correction in: *FEBS Lett.* **441**, 342 (1998).
7. P. N. Panton, F. C. O. Valentine, Staphylococcal toxin. *Lancet* **1**, 506–508 (1932).
8. C. L. Ventura *et al.*, Identification of a novel *Staphylococcus aureus* two-component leukotoxin using cell surface proteomics. *PLoS One* **5**, e11634 (2010).
9. R. Wang *et al.*, Identification of novel cytolytic peptides as key virulence determinants for community-associated MRSA. *Nat. Med.* **13**, 1510–1514 (2007).
10. C. J. de Haas *et al.*, Chemotaxis inhibitory protein of *Staphylococcus aureus*, a bacterial antiinflammatory agent. *J. Exp. Med.* **199**, 687–695 (2004).
11. A. L. DuMont *et al.*, *Staphylococcus aureus* LukAB cytotoxin kills human neutrophils by targeting the CD11b subunit of the integrin Mac-1. *Proc. Natl. Acad. Sci. U.S.A.* **110**, 10794–10799 (2013).
12. I. Jongerius *et al.*, Staphylococcal complement evasion by various convertase-blocking molecules. *J. Exp. Med.* **204**, 2461–2471 (2007).
13. D. Patel, B. D. Wines, R. J. Langley, J. D. Fraser, Specificity of staphylococcal superantigen-like protein 10 toward the human IgG1 Fc domain. *J. Immunol.* **184**, 6283–6292 (2010).
14. W. Salgado-Pabón, P. M. Schlievert, Models matter: The search for an effective *Staphylococcus aureus* vaccine. *Nat. Rev. Microbiol.* **12**, 585–591 (2014).
15. H. Buvelot, K. M. Posfay-Barbe, P. Linder, J. Schrenzel, K. H. Krause, *Staphylococcus aureus*, phagocyte NADPH oxidase and chronic granulomatous disease. *FEMS Microbiol. Rev.* **41**, 139–157 (2017).
16. S. Bhakdi, M. Muhly, S. Korom, F. Hugo, Release of interleukin-1 beta associated with potent cytocidal action of staphylococcal alpha-toxin on human monocytes. *Infect. Immun.* **57**, 3512–3519 (1989).
17. F. Alonzo III *et al.*, *Staphylococcus aureus* leucocidin ED contributes to systemic infection by targeting neutrophils and promoting bacterial growth in vivo. *Mol. Microbiol.* **83**, 423–435 (2012).
18. F. Alonzo III *et al.*, CCR5 is a receptor for *Staphylococcus aureus* leukotoxin ED. *Nature* **493**, 51–55 (2013).
19. K. M. Boguslawski *et al.*, Exploiting species specificity to understand the tropism of a human-specific toxin. *Sci. Adv.* **6**, eaax7515 (2020).
20. K. Tam *et al.*, Targeting leukocidin-mediated immune evasion protects mice from *Staphylococcus aureus* bacteremia. *J. Exp. Med.* **217**, e20190541 (2020).
21. S. S. Perelman *et al.*, Genetic variation of staphylococcal LukAB toxin determines receptor tropism. *Nat. Microbiol.* **6**, 731–745 (2021).
22. D. Duffy *et al.*; Multinational FOCIS Centers of Excellence, Standardized whole blood stimulation improves immunomonitoring of induced immune responses in multi-center study. *Clin. Immunol.* **183**, 325–335 (2017).
23. E. W. Skjeflo, D. Christiansen, T. Espevik, E. W. Nielsen, T. E. Mollnes, Combined inhibition of complement and CD14 efficiently attenuated the inflammatory response induced by *Staphylococcus aureus* in a human whole blood model. *J. Immunol.* **192**, 2857–2864 (2014).
24. A. T. Giraudo, C. G. Raspanti, A. Calzolari, R. Nagel, Characterization of a Tn551-mutant of *Staphylococcus aureus* defective in the production of several exoproteins. *Can. J. Microbiol.* **40**, 677–681 (1994).
25. K. Rogasch *et al.*, Influence of the two-component system SaeRS on global gene expression in two different *Staphylococcus aureus* strains. *J. Bacteriol.* **188**, 7742–7758 (2006).
26. L. Thomer *et al.*, Antibodies against a secreted product of *Staphylococcus aureus* trigger phagocytic killing. *J. Exp. Med.* **213**, 293–301 (2016).
27. T. K. Nygaard *et al.*, SaeR binds a consensus sequence within virulence gene promoters to advance USA300 pathogenesis. *J. Infect. Dis.* **201**, 241–254 (2010).
28. F. Sun *et al.*, In the *Staphylococcus aureus* two-component system sae, the response regulator SaeR binds to a direct repeat sequence and DNA binding requires phosphorylation by the sensor kinase SaeS. *J. Bacteriol.* **192**, 2111–2127 (2010).
29. Y. Liu *et al.*, Contribution of coagulase and its regulator SaeRS to lethality of CA-MRSA 923 bacteremia. *Pathogens* **10**, 1396 (2021).
30. U. Trivedi *et al.*, *Staphylococcus aureus* coagulases are exploitable yet stable public goods in clinically relevant conditions. *Proc. Natl. Acad. Sci. U.S.A.* **115**, E11771–E11779 (2018).
31. R. Banchereau *et al.*, Host immune transcriptional profiles reflect the variability in clinical disease manifestations in patients with *Staphylococcus aureus* infections. *PLoS One* **7**, e34390 (2012).
32. X. Hu, J. Yu, S. D. Crosby, G. A. Storch, Gene expression profiles in febrile children with defined viral and bacterial infection. *Proc. Natl. Acad. Sci. U.S.A.* **110**, 12792–12797 (2013).
33. M. Uguccioni, M. D'Apuzzo, M. Loetscher, B. Dewald, M. Baggiolini, Actions of the chemotactic cytokines MCP-1, MCP-2, MCP-3, RANTES, MIP-1 alpha and MIP-1 beta on human monocytes. *Eur. J. Immunol.* **25**, 64–68 (1995).
34. R. Porat, D. D. Poutsiaka, L. C. Miller, E. V. Granowitz, C. A. Dinarello, Interleukin-1 (IL-1) receptor blockade reduces endotoxin and Borrelia burgdorferi-stimulated IL-8 synthesis in human mononuclear cells. *FASEB J.* **6**, 2482–2486 (1992).
35. E. W. Sward *et al.*, *Staphylococcus aureus* SaeR/S-regulated factors decrease monocyte-derived tumor necrosis factor-α to reduce neutrophil bactericidal activity. *J. Infect. Dis.* **217**, 943–952 (2018).
36. A. H. Chan, K. Schroder, Inflammasome signaling and regulation of interleukin-1 family cytokines. *J. Exp. Med.* **217**, e20190314 (2020).
37. S. J. Klebanoff *et al.*, Stimulation of neutrophils by tumor necrosis factor. *J. Immunol.* **136**, 4220–4225 (1986).
38. M. Baggiolini, A. Walz, S. L. Kunkel, Neutrophil-activating peptide-1/interleukin 8, a novel cytokine that activates neutrophils. *J. Clin. Invest.* **84**, 1045–1049 (1989).
39. F. Liao *et al.*, Human Mig chemokine: Biochemical and functional characterization. *J. Exp. Med.* **182**, 1301–1314 (1995).
40. C. A. Dinarello, Biologic basis for interleukin-1 in disease. *Blood* **87**, 2095–2147 (1996).
41. P. Jayaraman *et al.*, IL-1β promotes antimicrobial immunity in macrophages by regulating TNFR signaling and caspase-3 activation. *J. Immunol.* **190**, 4196–4204 (2013).
42. S. Rose-John, K. Winthrop, L. Calabrese, The role of IL-6 in host defence against infections: Immunobiology and clinical implications. *Nat. Rev. Rheumatol.* **13**, 399–409 (2017).
43. S. D. Kobayashi *et al.*, Rapid neutrophil destruction following phagocytosis of *Staphylococcus aureus*. *J. Innate Immun.* **2**, 560–575 (2010).
44. O. L. Brekke *et al.*, Combined inhibition of complement and CD14 abolish *E. coli*-induced cytokine-, chemokine- and growth factor-synthesis in human whole blood. *Mol. Immunol.* **45**, 3804–3813 (2008).
45. K. M. Kengatharan, S. De Kimpe, C. Robson, S. J. Foster, C. Thiemermann, Mechanism of gram-positive shock: Identification of peptidoglycan and lipoteichoic acid moieties essential in the induction of nitric oxide synthase, shock, and multiple organ failure. *J. Exp. Med.* **188**, 305–315 (1998).

46. E. Mattsson, T. Hartung, S. Morath, A. Egesten, Highly purified lipoteichoic acid from *Staphylococcus aureus* induces procoagulant activity and tissue factor expression in human monocytes but is a weak inducer in whole blood: Comparison with peptidoglycan. *Infect. Immun.* **72**, 4322–4326 (2004).
47. N. Malachowa *et al.*, Global changes in *Staphylococcus aureus* gene expression in human blood. *PLoS One* **6**, e18617 (2011).
48. M. Cruciani *et al.*, Differential responses of human dendritic cells to live or inactivated *Staphylococcus aureus*: Impact on cytokine production and T helper expansion. *Front. Immunol.* **10**, 2622 (2019).
49. J. Moretti *et al.*, STING senses microbial viability to orchestrate stress-mediated autophagy of the endoplasmic reticulum. *Cell* **171**, 809–823.e13 (2017).
50. R. P. Novick, D. Jiang, The staphylococcal saeRS system coordinates environmental signals with agr quorum sensing. *Microbiology (Reading)* **149**, 2709–2717 (2003).
51. H. Cho *et al.*, Calprotectin increases the activity of the SaeRS two component system and murine mortality during *Staphylococcus aureus* infections. *PLoS Pathog.* **11**, e1005026 (2015).
52. T. Geiger, C. Goerke, M. Mainiero, D. Kraus, C. Wolz, The virulence regulator Sae of *Staphylococcus aureus*: Promoter activities and response to phagocytosis-related signals. *J. Bacteriol.* **190**, 3419–3428 (2008).
53. M. A. Benson, S. Lilo, T. Nygaard, J. M. Voyich, V. J. Torres, Rot and SaeRS cooperate to activate expression of the staphylococcal superantigen-like exoproteins. *J. Bacteriol.* **194**, 4355–4365 (2012).
54. Q. Liu, W. S. Yeo, T. Bae, The SaeRS Two-Component System of *Staphylococcus aureus*. *Genes (Basel)* **7**, 81 (2016).
55. J. R. Chapman *et al.*, Using quantitative spectrometry to understand the influence of genetics and nutritional perturbations on the virulence potential of *Staphylococcus aureus*. *Mol. Cell. Proteomics* **16** (4 suppl. 1), S15–S28 (2017).
56. B. R. Boles, M. Thoendel, A. J. Roth, A. R. Horswill, Identification of genes involved in polysaccharide-independent *Staphylococcus aureus* biofilm formation. *PLoS One* **5**, e10146 (2010).
57. E. T. Berends *et al.*, Distinct localization of the complement C5b-9 complex on Gram-positive bacteria. *Cell. Microbiol.* **15**, 1955–1968 (2013).
58. T. Reyes-Robles, A. Lubkin, F. Alonzo III, D. B. Lacy, V. J. Torres, Exploiting dominant-negative toxins to combat *Staphylococcus aureus* pathogenesis. *EMBO Rep.* **17**, 780 (2016).
59. T. Hashimshony *et al.*, CEL-Seq2: Sensitive highly-multiplexed single-cell RNA-Seq. *Genome Biol.* **17**, 77 (2016).
60. B. Langmead, S. L. Salzberg, Fast gapped-read alignment with Bowtie 2. *Nat. Methods* **9**, 357–359 (2012).
61. S. Anders, P. T. Pyl, W. Huber, HTSeq–a Python framework to work with high-throughput sequencing data. *Bioinformatics* **31**, 166–169 (2015).
62. M. I. Love, W. Huber, S. Anders, Moderated estimation of fold change and dispersion for RNA-seq data with DESeq2. *Genome Biol.* **15**, 550 (2014).
63. M. D. Young, M. J. Wakefield, G. K. Smyth, A. Oshlack, Gene ontology analysis for RNA-seq: Accounting for selection bias. *Genome Biol.* **11**, R14 (2010).
64. M. E. Ritchie *et al.*, limma powers differential expression analyses for RNA-sequencing and microarray studies. *Nucleic Acids Res.* **43**, e47 (2015).
65. H. Wickham, *ggplot2: Elegant Graphics for Data Analysis* (Springer-Verlag, New York, NY, 2016).
66. Z. Gu, R. Eils, M. Schlesner, Complex heatmaps reveal patterns and correlations in multidimensional genomic data. *Bioinformatics* **32**, 2847–2849 (2016).
67. C. H. Gao, G. Yu, P. Cai, ggVennDiagram: An intuitive, easy-to-use, and highly customizable R package to generate Venn diagram. *Front. Genet.* **12**, 706907 (2021).
68. A. J. Iqbal *et al.*, A real time chemotaxis assay unveils unique migratory profiles amongst different primary murine macrophages. *PLoS One* **8**, e58744 (2013).
69. E. E. Zwack *et al.*, Staphylococcus aureus induces a muted host response in human blood that blunts the recruitment of neutrophils. GEO. https://www.ncbi.nlm.nih.gov/geo/query/acc.cgi?acc=GSE193219. Deposited 7 January 2022.
70. J. C. Devlin, E. E. Zwack, P. Loke, V. J. Torres, Deconvolution of myeloid cell cytokine specific transcriptional profiles during tuberculosis and cancer identifies neutrophil activation as a prognostic feature [cultured cells]. GEO. https://www.ncbi.nlm.nih.gov/geo/query/acc.cgi?acc=GSE131990. Deposited 30 May 2019.
71. R. Hu, J. Yu, S. Crosby, G. A. Storch, Whole blood transcriptional signature distinguishes viral infection from bacterial infection in febrile young children. GEO. https://www.ncbi.nlm.nih.gov/geo/query/acc.cgi?acc=GSE40396. Accessed 3 January 2020.
72. R. Banchereau, O. Ramilo, Genome-wide analysis of whole blood transcriptional response to community-acquired Staphylococcus aureus infection in vivo. GEO. https://www.ncbi.nlm.nih.gov/geo/query/acc.cgi?acc=GSE30119. Accessed 6 December 2020.